# MORPHOLOGY EFFECTS ON CONSTITUTIVE PROPERTIES OF FOAMS

J. Köll*, S. Hallström

Department of Aeronautical and Vehicle Engineering, KTH Royal Institute of Technology, Stockholm, Sweden

* Corresponding author (koll@kth.se)

**Keywords**: *Rigid foam, morphology, mechanical properties, stochastic modeling*

## 1 Introduction

Low-density rigid foams are commonly used as core materials in sandwich structures. Such foams are here modeled as stochastic Voronoi partitions of 3D space that are meshed and analyzed with finite elements (FE). The constitutive properties and their relation to morphological variations in the cellular structures are studied, especially how the stiffness of the foam models varies with respect to a number of characteristic measures of the foam structure.

Various models of cellular materials have been used in the past, ranging from quite simplistic to very advanced geometrical representations. Strongly idealized models of single cells can be used to provide certain scaling laws of foams [1] and there are a few polyhedral unit-cells that are space-filling. However, they all compromise some of the properties that characterize real foam materials, such as connectivity or global isotropy. To increase authenticity, computer tomography has also been used to depict the true three-dimensional geometry of small samples of foams. They have then been digitally recreated and used for FE analysis [2]. Such models are amorphous and very representative but provide only relatively small samples from a big variety of cell constellations. These models are neither regular nor periodic, which cause great challenges in analysis since adequate loads and boundary conditions are difficult to apply. Another way of increasing authenticity is to generate random and isotropic structures that resemble real foams [3]. Previous work has shown not only that input parameters and choice of different methods for generating stochastic cellular structures can be related to statistical measures on the morphology, but also that the methodology needs to be quite sophisticated for the models to accurately resemble dry foams [4].

The scope of this work is to investigate if the level of model sophistication also affects the resulting homogenized mechanical properties.

## 2 Modeling and simulations

The approach is to develop a methodology for generating realistic computer models that are structurally and mechanically representative of true foam materials. They should capture the random, amorphous nature of real foam materials for which the cell shapes and sizes vary significantly.

The cellular microstructure is modeled as a representative volume element (RVE) containing numerous disordered cells. The RVEs should be large enough to be globally representative of the modeled materials. For systematic handling of loads and boundary conditions spatially periodic RVEs, containing fifty cells each, were built. Bulk material properties were assigned to the cell walls. The homogenized constitutive properties of the foam models were then determined with FE analysis, applying periodic boundary conditions to make the models artificially continuous.

The RVEs vary in shape but are always of unit volume. The individual cells vary both in shape and size. The cells are space filling without overlap, and define the exact shape of the RVE. An example of a random disordered polydisperse model with 50 cells is shown in fig. 1.

### 2.1 Voronoi partitioning

The subdivision of the RVE into cells was made as a Voronoi partitioning. A three dimensional Voronoi partitioning is based on a set of seed points distributed in a model space $\Omega$. The Voronoi partition or region $V_i$ associated with seed point $i$ is given by

$$V_i = \left\{ \overline{x} \in \Omega \mid \|\overline{x} - \overline{x}_i\| \le \|\overline{x} - \overline{x}_j\|, i \neq j \right\} \quad (1)$$

where $\overline{x}_i$ and $\overline{x}_j$ are the coordinates of seed points $i$ and $j$ respectively. This means that every seed point is surrounded by one cell, and the cell contains all points in space that are closer to this particular seed point than to any other. To obtain spatially periodic models the partitioning is made in a spatially periodic environment, i.e. the model space is surrounded by copies of itself. To create disordered structures, the seed points must be randomly distributed in the space $\Omega$.

## 2.2 Seed point distributions

Generating random points within the model space without any further constraints will result in a geometry with extreme variation in both cell size and shape, which does not resemble the structure of real foams. To obtain more foam-like geometries an algorithm preventing seed points to end up too close to each other, was used. Two different methods based on packing of hard spheres were tested and evaluated with regard to morphological and mechanical properties.

The two methods for generating random seed point distributions were Random Sequential Adsorption (RSA) and Random Close Packing (RCP). Both methods generate packings of equal-sized hard spheres where the sphere centers constitute seed points for the Voronoi partitioning.

RSA is a fairly simple way to generate sphere packings. Spheres are randomly, sequentially and irreversibly deposited in the model space where possible without overlap. RSA generates relatively loose packings with $\phi \le 0.36$, where $\phi$ is defined as the volume fraction of spheres in the model space. RCP is usually generated using "molecular dynamics" simulations, i.e. based on interaction between particles or spheres. Typically a separating force spreads the particles or spheres in the model space until equilibrium is achieved. RCP enables relatively dense packings with $\phi \le 0.64$.

All RCP distributions used in the work presented here were generated with a Python-language implementation of Jodrey and Tory's algorithm [5,6]. Several ideas for reducing computational time were found in Bargiel and Moscinski's C-language implementation of the same algorithm [7].

## 2.3 Distribution of solid

Each model was given a prescribed relative density by controlling the wall thickness of the cells. In real foams the bulk material is typically somewhat concentrated along the cell wall edges, and the thickness varies over the cell faces. As a first approximation the material in the models was evenly distributed, i.e. all cell walls were given equal and uniform thickness and no additional material was added at the cell wall edges. Note however that the shell elements in the model inherently have small overlaps at the cell edges.

## 2.4 Stiffness analysis

The stiffness of the models was determined by FE analysis. Bulk material properties were assigned to cell walls that were modeled with shell elements. Prescribed uniform global strains were applied to the models together with periodic boundary conditions. The reaction forces and the lateral contractions were determined and the stiffness parameters were calculated from principles of elasticity. The full orthotropic stiffness matrix was extracted for each model.

## 3  Results

32 models consisting of 50 cells each were generated and analyzed. Half of the models were based on RSA distributions and half on RCP distributions. In addition 5 models based on RCP distributions consisting of 350 cells each were generated. For these 5 models only the stiffness was evaluated for comparison.

## 3.1 Morphology

The morphology of totally 1600 cells was evaluated. The normalized cell volume distributions look relatively symmetric. As can be seen in fig. 2 the distribution is significantly narrower for the RCP models than for the RSA models, which show a broader variation in cell volume. This is an expected result related to the higher packing fraction of spheres in the RCP distribution.

The normalized face area distributions shown in fig. 3 reveal interesting characteristics of the Voronoi structures. The RSA models demonstrate a surprisingly high content of very small faces. As might be expected, the RCP models show an

increase in mid-sized faces while there are fewer small and large faces. The largest faces present in the RSA structures are not to be found in the RCP structures. At the same time the peak for very small faces remains, even if it is less pronounced.

Fig. 4 shows the normalized edge length distribution of the cell walls. The trends are similar as for the face area distributions, although not as strong. Both models show a high occurrence of short edges but in contrast to the faces no peaks are visible.

The RCP structures have an average number of faces/cell $<F> = 14.2$ compared to $<F> = 14.9$ for the RSA structures. For monodisperse soap froth, Matzke studied 600 cells and reported $<F> = 13.7$ [8]. Fig. 5 shows the occurrence of cells with $F$ faces for RSA and RCP models together with Matzkes experimental results. The average number of faces/cell $<F>$ and the average number of edges/face $<n>$ are coupled through the relation $<n>=6-12/<F>$ [1].

### 3.2 Constitutive properties

For each 50-cell model 6 Poisson's ratios $\nu_{ij}$ were extracted from 3 different load cases. Fig. 6 shows the results as function of relative density. The Poisson's ratio seems to decrease slightly with increasing relative density. A bulk material Poisson's ratio $\nu_s=0.3$ was assumed in all models.

The linear elastic stiffness of all 50-cell models was evaluated in 3 orthogonal directions and for 4 different relative densities. In Fig. 7 the extracted relative Young's and shear moduli are presented for different relative densities. The relations may appear to be linearly dependent but a closer inspection reveals that the relation is slightly non-linear. Note also that the figure shows four curves and not two. There is no significant difference in the predicted stiffness from the RSA and RCP despite the morphological differences shown in Figs. 2-5. Quadratic polynomials were fitted to the data on the form

$$\frac{E^*}{E_s} = C_1 \left( \frac{\delta^*}{\delta_s} \right)^2 + C_2 \frac{\delta^*}{\delta_s} \qquad (2)$$

$$\frac{G^*}{E_s} = C_3 \left( \frac{\delta^*}{\delta_s} \right)^2 + C_4 \frac{\delta^*}{\delta_s} \qquad (3)$$

where the coefficients $C_1$-$C_4$ given in Table 1 express the non-linear relations between relative density and relative moduli.

Despite the random nature of the structures the spread in results within each model category is extremely small. The error-bars indicating the standard deviation of the results in Fig. 7 can hardly be detected in the graph. The relative standard deviation for the predicted Young's modulus is <1% for RSA models and <0.5% for RCP models. The difference between the mean predicted Young's modulus for RSA and RCP models is <1%. Fig. 7 also shows the data for the 350-cell models. For visualization reasons the results were calculated for other relative densities. The results closely match the ones for the 50-cell models, with almost identical coefficients $C_1$-$C_4$ (Table 1).

### 4 Discussion and Conclusions

Both model types show a slightly non-linear relation between the relative modulus and the relative density in the investigated range (Fig. 7). The influence from the slightly overlapping shell elements has not been distinguished. The difference in morphology between RSA an RCP models (Fig. 2-5) is significant but does not affect the extracted stiffness parameters. The small standard deviation in the predicted stiffness for both RSA and RCP models indicates that the models are isotropic, which is also confirmed by individual moduli values from different material directions. The results generally indicate that the number of cells in the RVEs is sufficient to provide consistent results, also confirmed by the nearly identical results for the 350-cell models.

When running FE the high occurrence of short edges and small faces (Fig. 3,4) makes meshing problematic. The quality of the mesh can be compromised by a big variation in both element size and internal element angles. The problem concerns both model types but is more evident for RSA models.

### 5 Future work

The effects from introducing different distributions of solid are not yet investigated but intended to be included in coming work. The work presented here

has only focused on the stiffness in the linear elastic regime. Nonlinear effects and the response at large deformations have not yet been investigated.

It has been shown that cellular morphology is in better agreement with Matzke's results after minimizing the surface area of the Voronoi structure [4]. This minimization of area introduces curvature to both cell edges and faces. Such curvature will likely also affect the stiffness of the cell walls.

Table 1. Coefficients fitted to eq. 2 and 3.

|        | RSA 50 cells | RCP 50 cells | RCP 350 cells |
|--------|--------------|--------------|---------------|
| $C_1$  | 0.11         | 0.11         | 0.11          |
| $C_2$  | 0.35         | 0.34         | 0.34          |
| $C_3$  | 0.052        | 0.053        | 0.051         |
| $C_4$  | 0.12         | 0.12         | 0.12          |
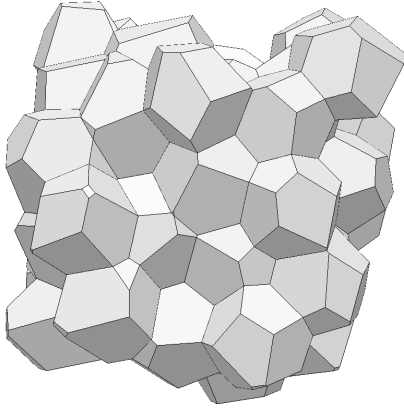


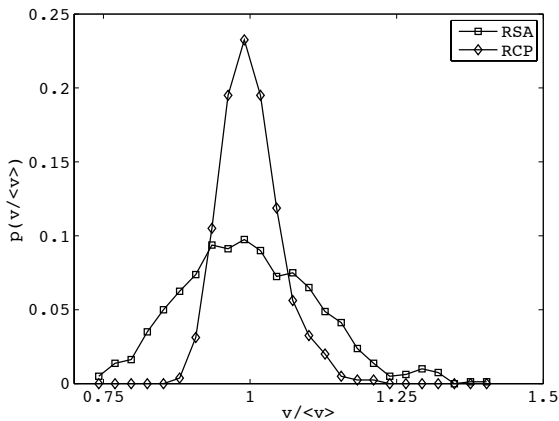Fig.1. Example of a spatially periodic computer model consisting of 50 random cells (RCP).



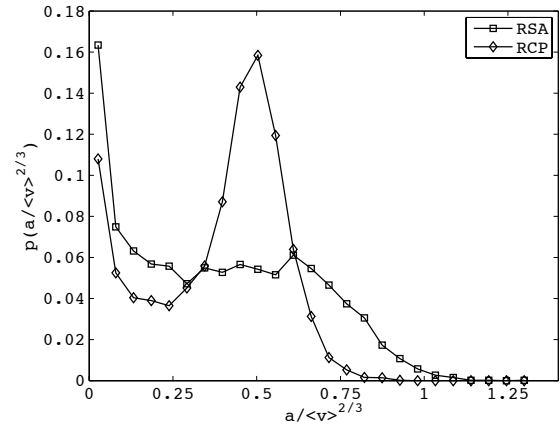Fig.2. Cell volume distribution normalized with the average cell volume $\langle v \rangle$.



Fig.3. Face area distribution normalized with $\langle v \rangle^{2/3}$ where $\langle v \rangle$ is the average cell volume.
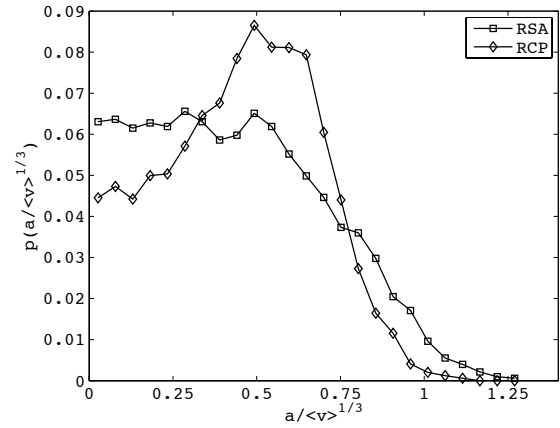


Fig.4. Edge length distribution normalized with $\langle v \rangle^{1/3}$ where $\langle v \rangle$ is the average cell volume.
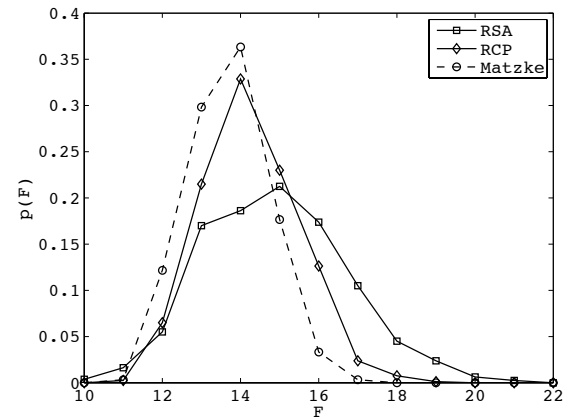


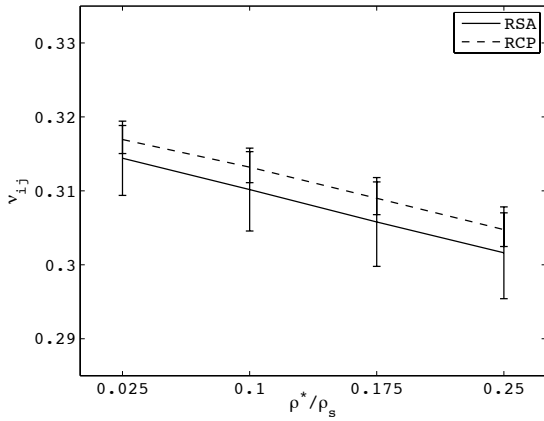Fig.5. The occurrence of cells with F faces compared with Matzke's experimental results.

Fig.6. Predicted Poisson's ratio with error bars indicating the standard deviation.
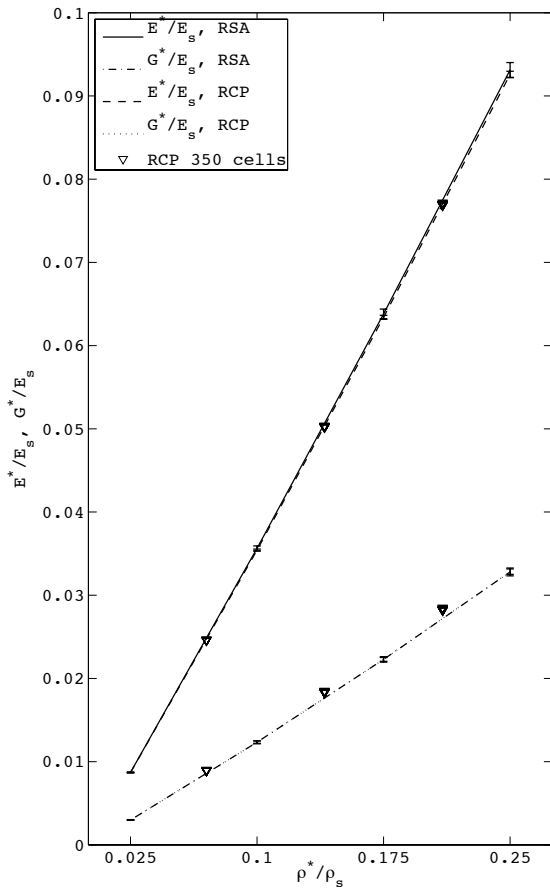


Fig.7. Predicted relative modulus with error bars indicating the standard deviation. Data from five 350-cell models is also shown for reference.

**References**

[1] L.J. Gibson and M.F. Ashby "*Cellular Solids*". 2nd edition, Cambridge University Press, 1997.

[2] S. Youssef, E. Maire and R. Gaertner, "Finite element modeling of the actual structure of cellular materials determined by X-ray tomography". *Acta Materialia*, Vol. 53, pp 719-730, 2005.

[3] A.P. Roberts and E.J. Garboczi, "Elastic Moduli of Model Random Three-Dimensional Closed-Cell Cellular Solids". *Acta Materialia*, Vol. 49, pp 189-197, 2001

[4] A.M. Kraynik, "The Structure of Random Foam". *Advanced Engineering Materials*, Vol. 8, No. 9, pp 900-906, 2006.

[5] W.S. Jodrey and E.M Tory, "Computer simulation of close random packing of equal spheres". *Physical Review A*, Vol. 32, No. 4, pp 2347-2351, 1985

[6] W.S. Jodrey and E.M Tory, "Computer Simulation of Isotropic, Homogeneous, Dense Random Packing of Equal Spheres". *Powder Technology*, Vol. 30, pp 111-118, 1981

[7] M. Bargiel and J Moscinski, "C-language program for the irregular close packing of hard spheres". *Computer Physics Communications*, Vol 64, pp 183-192, 1991

[8] E.B. Matzke, "The Three-Dimensional Shape of Bubbles in Foam". *American Journal of Botany*, Vol. 33, pp 58-80, 1946